CHARACTERIZATION OF MECHANICAL PROPERTIES OF ALUMINIZED COATINGS IN ADVANCED GAS TURBINE BLADES USING A SMALL PUNCH METHOD

Y. Sugita, M. Ito,
Electric Power R & D Center
Chubu Electric Power Co.
Nagoya 458, Japan

S. Sakurai,
Mechanical Engineering Research Laboratory,
Hitachi Ltd.
Hitachi 317, Japan

T. E. Bloomer and J. Kameda
Ames Laboratory and Center for Advanced Technology Development
Iowa State University
Ames, IA 50011

ABSTRACT

This paper describes examination of the microstructure/composition and mechanical properties (22-950 °C) in aluminized CoCrAlY coatings of advanced gas turbine blades using scanning Auger microprobe and a small punch (SP) testing method. Aluminized coatings consisted of layered structure divided into four regimes; (I) Al enriched and Cr depleted region, (II) Al and Cr graded region, (III) fine grained microstructure with a mixture of Al and Cr enriched phases and (IV) Ni/Co interdifusion zone adjacent to the interface. SP specimens were prepared in order that the specimen surface would be located in the various coating regions. SP tests indicated strong dependence of the fracture properties on the various coatings regimes. Coatings I an II with very high microhardness showed much easier formation of brittle cracks in a wide temperature range, compared to coatings III and IV although the coating II had ductility improvement at 950 °C. The coating III had lower room temperature ductility than the coating IV. However, the ductility in the coating III exceeded that in the region IV above 730 °C due to a precipitous ductility increase. The integrity of aluminized coatings while in-service is discussed in light of the variation of the low cycle fatigue life as well as the ductility in the layered structure.

INTRODUCTION

Advanced technologies of superalloy casting and coatings enable one to enhance the performance of combined cycle gas turbines for electric power generation by increasing the firing temperature. The integrity of first stage blades, those subject to severe environmental attack and thermal stresses, becomes critical during the operation of gas turbines (Viswanathan and Allen, 1990, Sehitoglu, 1993). Aluminum packing treatments have been applied to improve the resistance of coatings to elevated temperature environmental attack in advanced gas turbine blades (Patnaik, 1994). While the formation of aluminum rich phases near the coating surface would mitigate the oxidation, the mechanical properties of aluminized coatings are inevitably deteriorated while in-service due to the microstructural evolution. There is a need to evaluate in-service mechanical degradation of blade coatings. However, the standard mechanical testing method is not suitable because the gas turbine blades possess a complex geometry and the coating degradation is localized in the near surface region. It has been recently shown (Sugita et al., 1995a, 1995b, Kameda et al., 1997) that in-service degradation of the mechanical properties and microstructure/composition in blade coatings can be well characterized using a small punch (SP) testing method in conjunction with scanning Auger microprobe (SAM) analysis.

This study is undertaken to examine the microstructure/composition and mechanical properties of aluminized CoCrAlY coatings over substrates made of directionally solidified nickel base superalloys in land-based gas turbine blades using the SAM analysis and SP method.

EXPERIMENTAL METHOD

This study employed gas turbine blades made of directionally solidified modified René 80 substrates and aluminized coatings (60.2%Co-30.6%Cr-8.9%Al-0.3% Y). The coating thickness varied in a range from 200-250 μm depending on the location of the blades.

As illustrated in Fig. 1, disk-shaped SP specimens (6 mm ϕ and 0.5 mm thick) were machined from the near surface region of blades. SAM specimens (3 mm wide, 2 mm thick and 10 mm long) along the longitudinal direction of blades were also extracted. The coating was located on a side of the SP and SAM specimens. The surface of coated SP specimens was placed in various coating regions indicated later. Substrate SP specimens were made by machining off the coatings.

DISCLAIMER

The surface of coated and substrate SP specimens was polished using emery paper (1000 grit) and/or alumina powders to eliminate the effect of the surface roughness and curvature on the mechanical properties (Kameda et al., 1996).

The microstructure and composition of the aluminized blades were examined by SAM. Longitudinal sections of the SAM specimen were sputter-cleaned (1.25 keV) in Ar gas atmosphere (5 x 10^{-6} Pa). The first derivative Auger peak height of various elements on the sputter-cleaned surfaces was acquired using a cylindrical mirror analyzer (5 keV) of Physical Electronics Model 660.

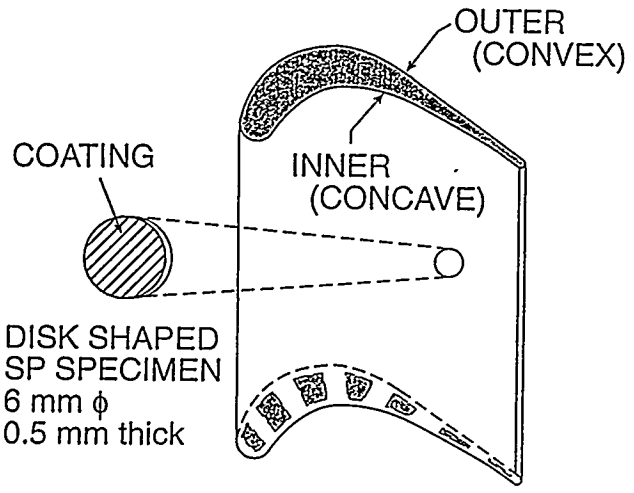

Figure 1. Extraction of disk-shaped small punch (SP) specimens from gas turbine blades.

The concentration of elements was estimated from the measured Auger signal intensity and the relative sensitivity factor of elements (Seah, 1983).

Specially designed specimen holders consisting of lower and upper dies and clamping screws were used for SP tests (Baik et al., 1983). Coated specimens were deformed using a puncher with a hemispherical tip (2.4 mm in diameter) to ensure that the coatings would be subject to tensile applied stresses. SP tests were carried out in air in a temperature range from 22-950 °C using a cross head speed of 8 x 10^{-5} m/s in a screw-driven Instron testing machine. The details of elevated temperature SP testing apparatus are indicated elsewhere (Sugita et al., 1995a). The cracking behavior of the aluminized coatings was examined using scanning electron microscopy (SEM).

RESULTS

Figure 2 depicts layered microstructure of the aluminized coatings. The layered microstructure was divided into four regimes designated as I-IV. Coatings I, II and IV had constant thickness of about 25 μm, 40 μm and 60 μm, respectively. The thickness of a coating III varied from 75 to 125 μm. The typical chemical compositions of the various coating regimes examined using SAM are shown in Figs. 3-6. The coating I observed near the coating surface had higher contents of Al and lower contents of Cr than the nominal ones (Fig. 3). Since the Co content did not much differ from the bulk, it is clear that Cr was replaced by Al during the aluminizing treatment. The coating I revealed grain coarsening to some extent (Kameda and Bloomer, 1996). The regime II had graded concentrations of Al and Cr. The compositions of the regime II adjacent to

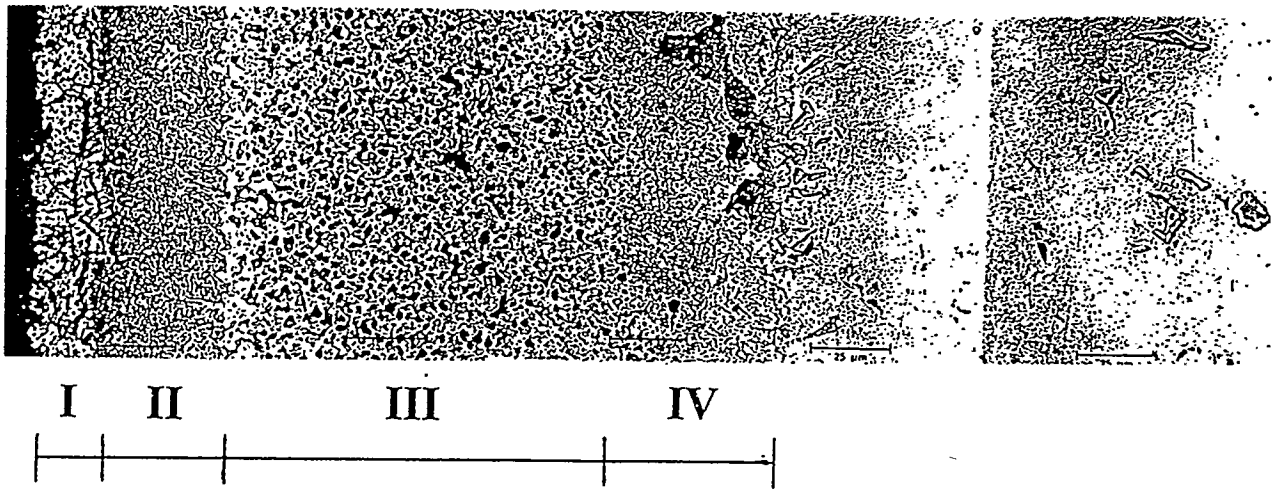

I: Al enriched and Cr depleted region
II: Al/Cr graded region
III: Al or Cr rich phase dispersed region
IV: Ni/Co diffusion region adjacent to interface

Figure 2. Micrograph indicating layered structure of aluminized coating divided into four regimes (I-IV).

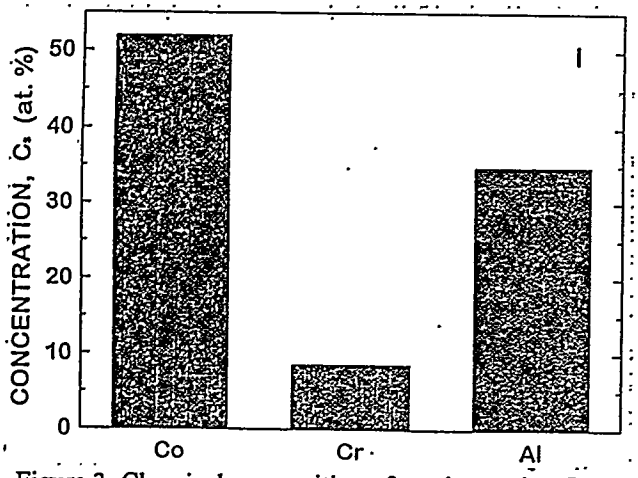

Figure 3. Chemical composition of coating regime I.

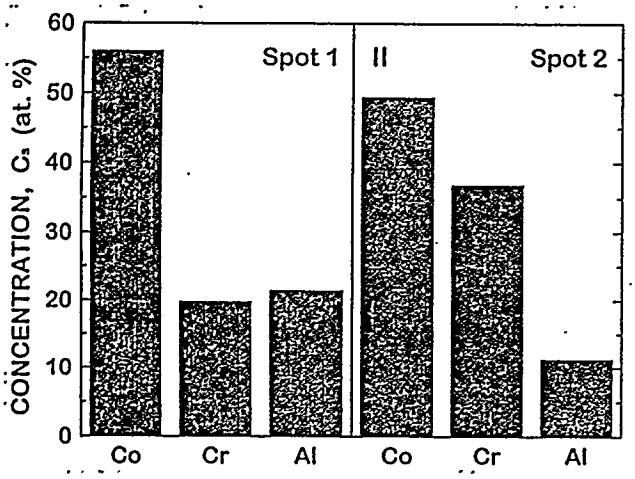

Figure 4. Chemical composition of coating regime II adjacent to I (spot 1) and III (spot 2).

the coatings I and III are indicated in spots 1 and 2, respectively, of Fig. 4. The interdifusion of Cr and Al is also evident with a slight change in the Co content. The regime III with fine grained microstructure had a mixture of Cr and Al enriched phases, as shown in Fig. 5 where the spot 1 indicates chemical compositions equivalent to the bulk one. The coating IV in the vicinity of the interface possessed a graded composition resulting from the interdiffusion of Co and Ni between the coating and substrate (Fig. 6). The spots 1 and 2 represent the compositions in the regions near the coating III and interface, respectively.

The mechanical properties of the various coating regimes were studied using the SP testing method. Several load vs. deflection curves obtained from coated SP specimen (I and III) tests at room temperature (RT) and 870 °C are indicated in Fig. 7. The yield load (P_y) can be defined at the transition point from the elastic to plastic bending deformation regime. The load was normalized by that in the coating III at RT. The yield strength (σ_y) in the blades was determined from the P_y value (Mao and Takahashi, 1987). The initiation of

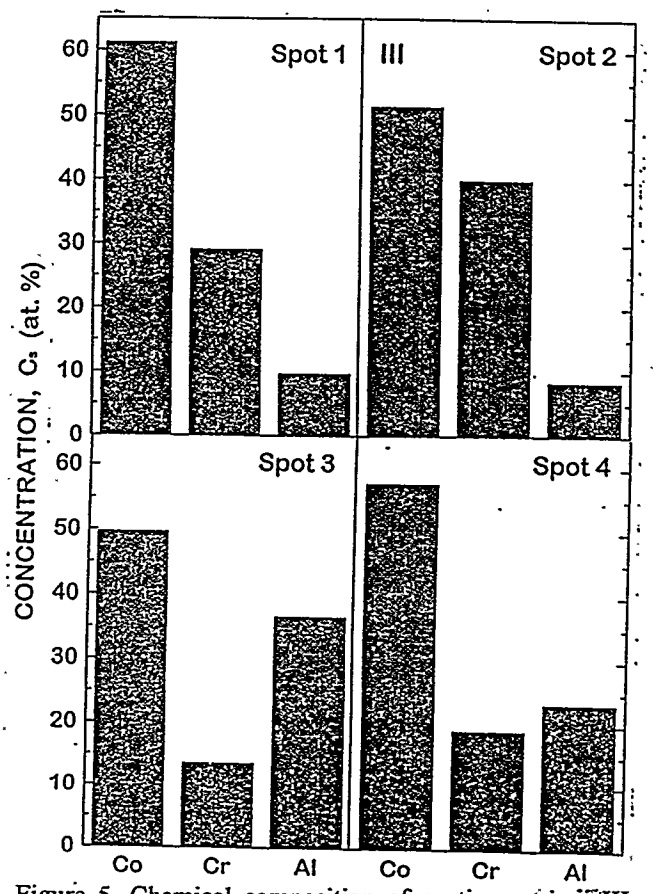

Figure 5. Chemical composition of coating regime III indicating Cr (spot 2) and Al (spots 3 & 4) enriched phases.

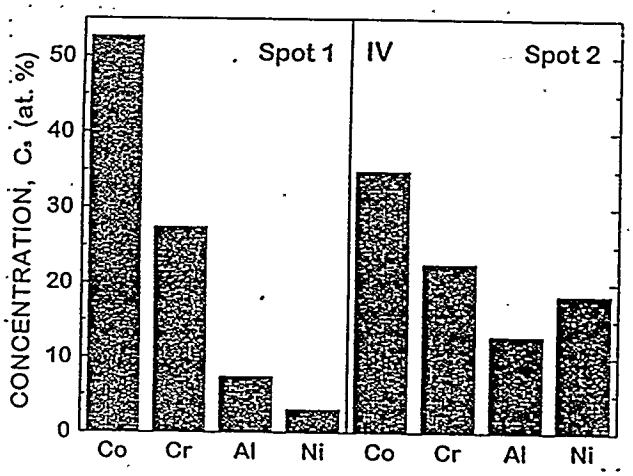

Figure 6. Chemical composition of coating regime IV adjacent to III (spot 1) and substrate (spot 2).

brittle cracks caused a decrease in the loading rate at the critical deflection (δ_f) (Fig. 7). In the coating I, brittle cracks formed easily at RT and 870 °C. Ductile cracking occurred in coating III tested at 870 °C without inducing a loading rate change (Fig. 7). In such cases,

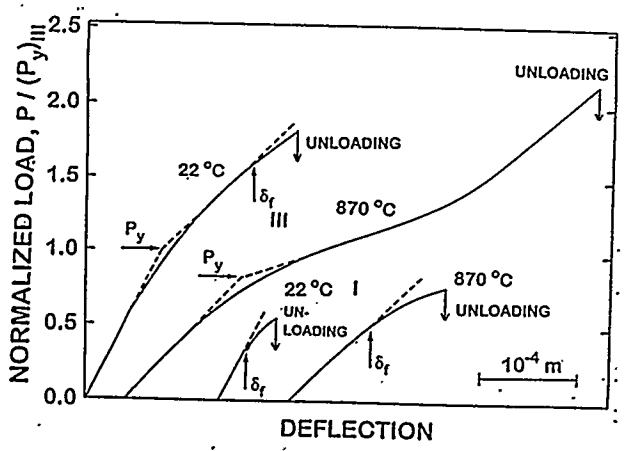

Figure 7. Load vs. deflection curves observed in coated SP specimens (I and III) tested at 22 °C and 870 °C indicating yield load (P_y) and critical deflection to cracking (δ_f). The load is normalized by yield load of III at RT.

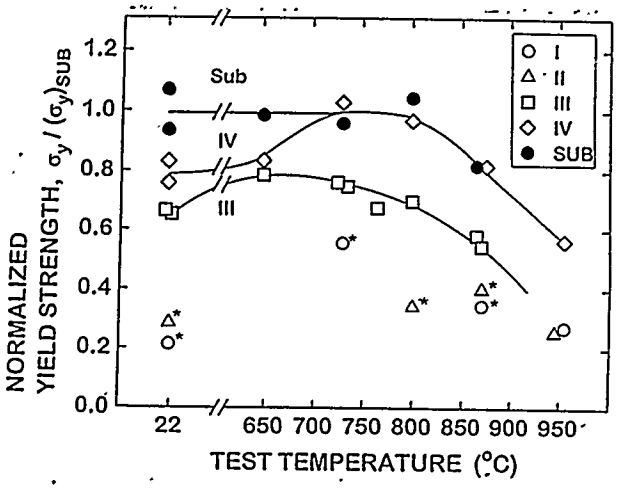

Figure 8. Temperature dependence of yield strength (σ_y) in coatings I, II, III and IV and substrate. The yield strength is normalized by that in substrate at RT.

load-interrupting SP tests were repeated at several deformation stages to determine the value of δ_f. The ductility (ε_f) of the coatings and substrates, defined at the crack initiation (Sugita et al., 1996a), was estimated from δ_f and the specimen thickness (Mao and Takahashi, 1987, Kameda and Mao, 1992).

The temperature dependence of σ_y, normalized by that in the substrate at RT, for the various coatings and substrate is shown in Fig. 8. Coated SP specimen (III and IV) tests indicated lower yield strength than substrate ones and strong dependence of σ_y on the coating regimes. In the substrate, the yield strength remained constant up to 800 °C and then started to drop. In the Al enriched coatings I and II, brittle cracks easily formed prior to the occurrence of plastic deformation. Thus the yield strength can not be determined for the coatings I and II. Instead, the fracture strength of the II is plotted in Fig. 8 (indicated by asterisk marks). As

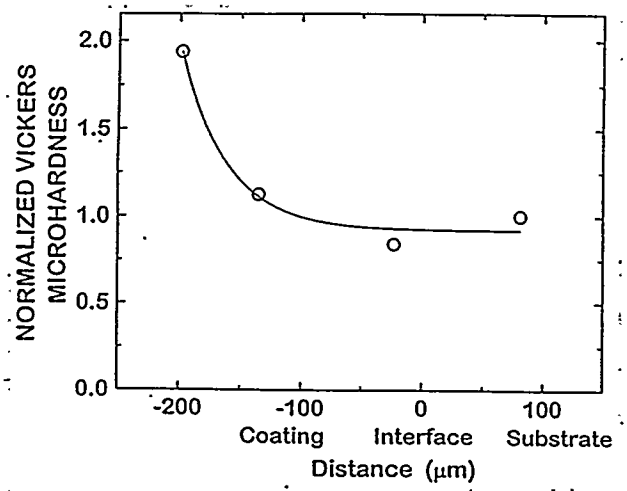

Figure 9. Variation of microhardness in aluminized coating and substrate. The microhardness is normalized by that in substrate.

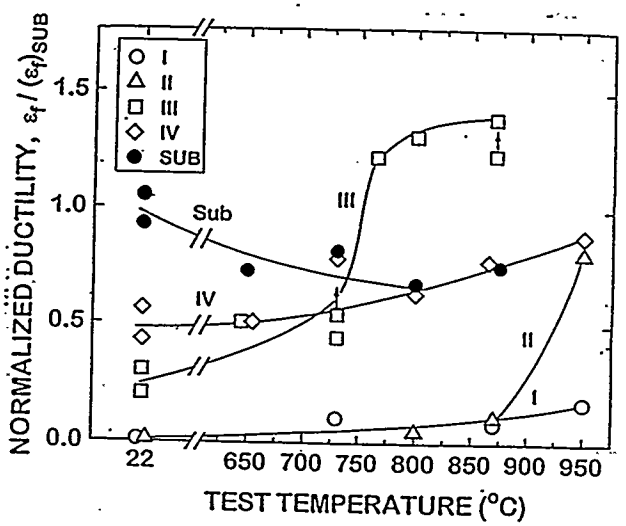

Figure 10. Temperature dependence of ductility (ε_f) in coatings I, II, III and IV and substrate. The ductility is normalized by that in substrate at RT.

shown in Fig. 9, it should be noted that near surface Al enriched coatings had much higher microhardness compared with the other coating regimes. The coating IV had higher yield strength than the regime III. The coatings III and IV showed hardening at 650-730 °C and 730-800 °C, respectively. The yield strength of the coating IV and substrate converged with each other above 730 °C.

The variations of the ductility to the testing temperature for the various coating regimes and substrates are illustrated in Fig. 10. The ductility was normalized by that in the coating III at RT. The substrate had the highest RT ductility and a ductility trough at 800 °C. The Al enriched coatings I and II showed very low ductility in a wide testing temperature range although the coating II had an increase in the

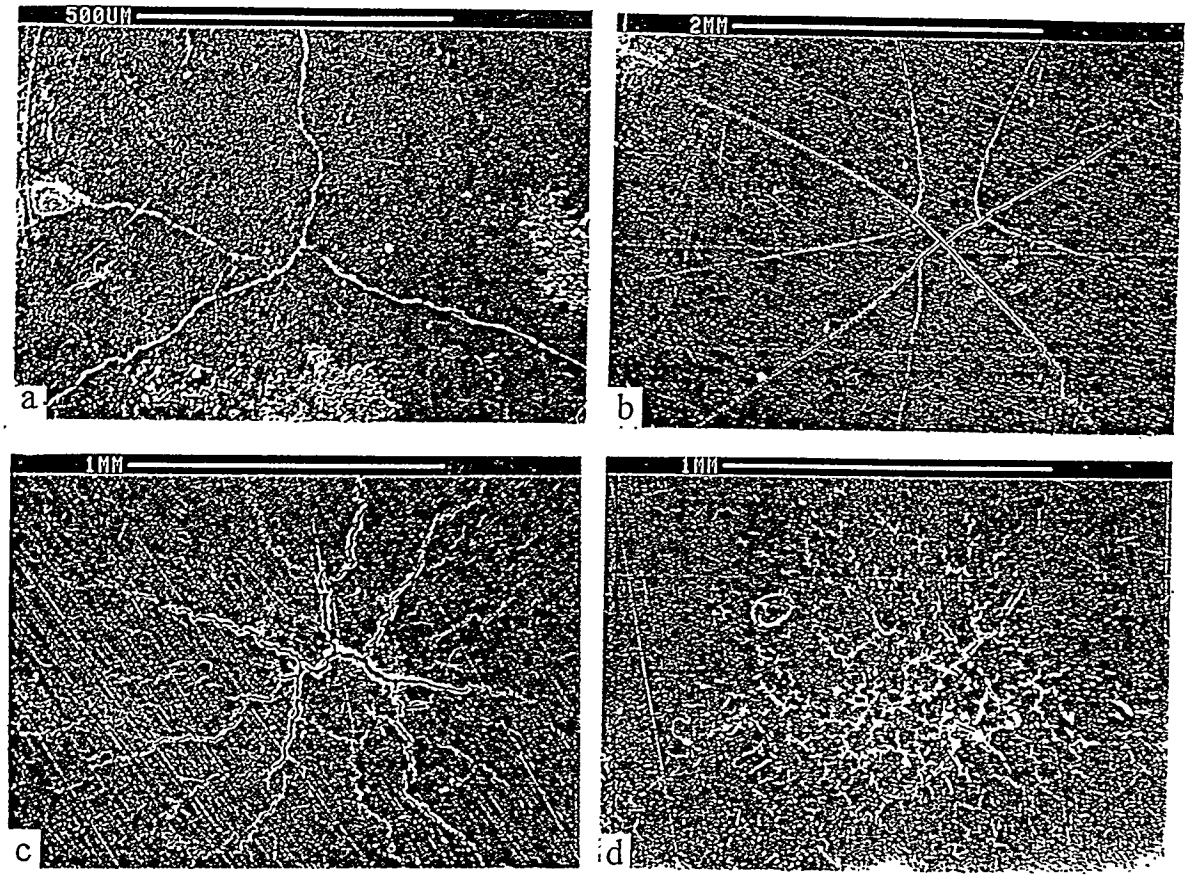

Figure 11. Cracking morphologies of coating regimes (a) I. (b) II. (c) III. and (d) IV tested at RT.

ductility at 950 °C. At RT, the coating IV containing Ni had a little higher ductility than the coating III with a mixture of Al and Cr enriched phases. The coating III had stronger temperature dependence of the ductility than the coating IV. Above 730 °C, the coating III had a precipitous increase in the ductility. The ductility in the coating IV converged with that in the substrate above 800 °C. From Fig. 10. it is clear that the substrate and coating IV containing Ni had better RT ductility than the other coating regimes without Ni. Conversely, the Ni containing substrate and coating IV had lower ductility at elevated temperatures compared to the coating III. This result is in agreement with that reported by Strang and Lang (1982).

The morphologies of cracking in coated SP specimens load-interrupted at RT and elevated temperatures were examined using SEM. Figure 11 exhibits a comparison of the RT cracking behavior observed in the various coating regimes. Brittle cracks initiated at the center of coated SP specimens. Nucleated brittle cracks in the coatings I-III predominantly propagated along the radial direction at RT while crack branching occurred in the coating IV. The density of cracks increased in the order of the coatings I-IV. The substrate showed more discrete nucleation of cracks at dispersed precipitates (Kameda and Bloomer, 1996). The cracking behavior of the coatings at 870 °C is shown in Fig. 12. The coating I revealed intergranular cracking. The coating II mainly fractured in a transgranular mode with a small mixture of intergranular cracking. Cracks discontinuously extended in the coatings III and IV. Furthermore, the coatings III and IV tested at 870 °C indicated more oxidation than the Al enriched coatings.

DISCUSSION

The present study has shown using the SP testing method that the aluminized coatings consisting of layered structure have wide variations in the temperature dependence of the yield strength and ductility. While the Al enriched coatings I and II would possess excellent resistance to elevated temperature environmental attack, brittle cracks readily form near the coating surface because of the low ductility. The engineering question is whether or not shallow cracks initiated near the surface would further extend into the regime III with higher ductility while in-service.

The allowance of coating cracks is related to the stress component in gas turbine blades. It is well known that the blade coatings of gas turbines are subject to larger thermal stresses produced by internal cooling than stresses applied by combustion gases. The tensile thermal stress is built up in the blade coatings in a certain temperature range during the start-up and shut-down transient operation of gas turbines, whereas the

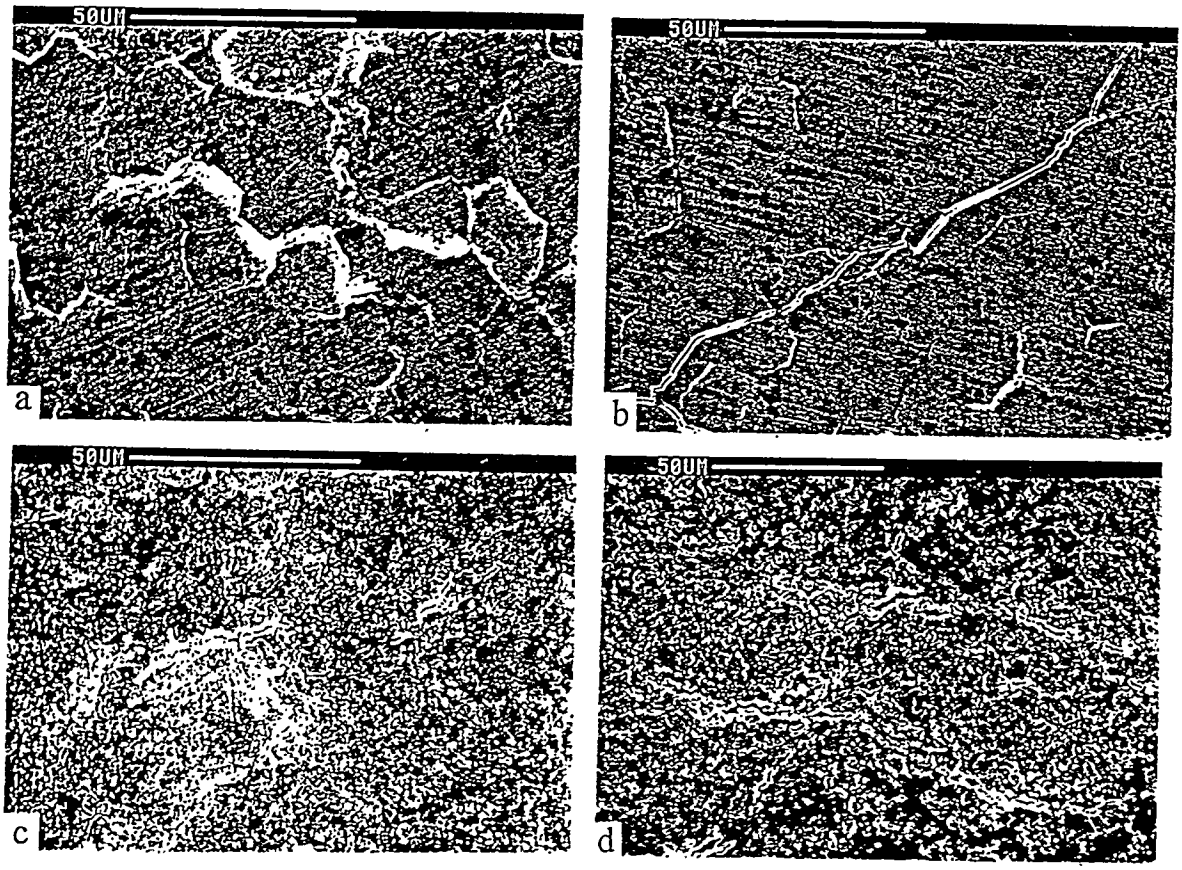

Figure 12 Cracking morphologies of coating regimes (a) I, (b) II, (c) III and (d) IV tested at 870 °C.

compressive thermal stress is mainly operative during the normal operation (Bernstein, 1993). However, the temperature distribution along rotating blades internally cooled has not yet been accurately evaluated (Cheruvu, et al., 1996). Thus, it is difficult to quantitatively estimate the maximum tensile stress and critical temperature range where the tensile thermal stress emerges in the coatings.

Combined cycle gas turbines in electric generating stations are frequently operated under the transient condition. The integrity of blade coatings is strongly controlled by the thermal fatigue behavior. The low cycle fatigue(LCF) behavior of the aluminized coatings at RT has been recently studied under constant displacement (Kameda and Bloomer, 1996). The LCF life in the coating I was much shorter, compared to that in the coating III, as expected from the RT ductility result. In addition, the coating III had more brittle cracking features and weaker dependence of the LCF life on the strain amplitude than CoNiCrAlY coatings although both the coatings had similar RT ductility (Sugita et al., 1996b, Kameda and Bloomer, 1996). A further study on the LCF behavior of the coating III at elevated temperatures will be required to ensure the crack tolerance under the transient operation.

Under the steady operation, the environmental attack resistance would play a more important role in degrading the blade coatings because the tensile thermal stress becomes minimal in the coatings. Kameda and Bloomer (1996) have shown that surface cracks formed in the coating I during short time creep tests in air at 870 °C are more preferentially oxidized, compared to the coating surface, due to the strong interaction of oxygen with dislocations. Thus there is a need to clarify how the localized oxidation near the crack tip affects the fracture properties at elevated temperature in the coating III

Regardless of the uncertainty of the tensile thermal stress, the critical temperature and the oxidizing effect, it is most likely that cracks formed near the coating surface would not grow much into the coating III with its high ductility at elevated temperatures. Moreover, the SP testing method in conjunction with the SAM analysis could be a useful tool to develop better coating constituents while compromising the oxidizing resistance and mechanical properties under monotonic and cyclic loading.

CONCLUSIONS

The microstructure/composition and mechanical properties in aluminized coatings of advanced gas turbine blades have been studied using scanning Auger microprobe and a small punch testing method. Aluminized coatings with layered structure were categorized by four regimes

depending on the microstructure and alloy composition; (I) Al enriched and Cr depleted region, (II) Al and Cr graded region, (III) fine grained region with Al or Cr enriched phases and (IV) Ni/Co interdifusion zone adjacent to the interface. Coated specimens of regimes III and IV indicated hardening at 650-800 °C. Coatings I an II with high microhardness showed easier formation of brittle cracks up to elevated temperatures than coatings III and IV although the ductility of the coating II increased at 950 °C. The coating III, compared to the region IV, had stronger temperature dependence of the ductility and better elevated temperature ductility. The effectiveness of aluminized coatings is discussed in light of the environmental attack resistance and mechanical performance.

ACKNOWLEDGMENTS

Ames Laboratory is operated for the US Department of Energy, Iowa State University under contract No. W-7405-ENG-82. The authors are grateful to A. H. Swansen and J. DeGabriele at Ames Laboratory for assistance on the experimental work.

REFERENCES

Viswanathan, R. and Allen, J. M., eds., 1990, *Life Assessment and Repair Technology for Combustion Turbine Hot Section Components*, ASM International, Materials Park, OH.

Sehitoglu, H., ed., 1993, *Thermomechanical Fatigue Behavior of Materials*, STP 1186, American Society for Testing Materials, Philadelphia, PA.

Patnaik, P. C., 1994, *Advances in High Temperature Structural Materials and Protective Coatings*, Koul, A. K., Parameswaran, V. R., Immarigeon, J. P. and Wallace, W., eds., National Research Council of Canada, Ottawa, p. 169.

Sugita, Y., Ito, M., Sakurai, S., Isobe, N., Gold, C. R., Bloomer, T. E. and Kameda, J., 1996a, *Materials and Manufacturing Processes*, Vol. 10, No. 5, p. 987.

Sugita, Y., Ito, M., Sakurai, S., Gold, C. R., Bloomer, T. E. and Kameda, J., 1996b, *Materials Ageing and Component Life Extension*, Bicego, V., Nitta, A. and Viswanathan, R., eds., EMAS, West Midland, p. 307.

Kameda, J., Bloomer, T. E., Sugita, Y., Ito, M. and Sakurai, S., 1997, *Materials Science and Engineering, A*, in press.

Kameda, J., Bloomer, T. E., Sugita, Y., Ito, M. and Sakurai, S., 1996, *Layered Materials for Structural Applications*, Lewandowski, J., Ward, C. H., Jackson, M. R. and Hunt, H. W., Jr., eds., Materials Research Society, Pittsburgh, p. 39.

Seah, M. P., 1983, *Practical Surface Analysis by Auger and X-Ray Photoelectron Spectroscopy*, Briggs, B. and Seah, M. P., eds., Willey, New York, NY, p. 181.

Baik, J. M., Kameda, J. and Buck, O., 1983, *Scripta Metallurgica*, Vol. 17, p. 1143.

Mao, X. and Takahashi, H., 1987, *Journal of Nuclear Materials*, Vol. 150, p. 42.

Kameda, J. and Mao, X., 1992, *Journal of Materials Science*, Vol. 27, p. 983.

Strang, A. and Lang, E., 1982, *High Temperature Alloys for Gas Turbines*, Brunetaud, R., Coutsouradis, D., Gibbons, T. B., Lindblom, Y., Meadowcroft, D. B. and Stickler, R., eds., Reidal Publishing Co. London, p. 469.

Kameda, J. and Bloomer, T. E., 1996, unpublished work, at Ames Laboratory and CATD, Iowa State University.

Bernstein, L. H., et al., 1993, *Thermomechanical Fatigue Behavior of Materials*, Sehitoglu, H., ed., STP 1186, American Society for Testing Materials, Philadelphia, PA, p. 212.

Cheruvu, N. S., Carr, T. J., Dworak, J. and Coyle, J., 1996, *JOM*, Vol. 48, No. 5, p. 34.